Multiple Bonding in the Chromium Dimer Supported by Two Diazadiene Ligands

Donald B. DuPré[†]

Department of Chemistry, University of Louisville, Louisville, Kentucky 40292

Received: October 3, 2008; Revised Manuscript Received: December 20, 2008

Analysis of the topology and delocalization of the electron density with the quantum theory of atoms in molecules (QTAIM) shows that the Cr_2 dimer when supported by two diazadiene ligands has a degree of bonding of 3.6—slightly less than that of a formal quadruple bond. The metal−ligand complex is held together by relatively weak dative bonds. Out-of-plane lone-pair-like charge concentrations on the nitrogen atoms are oriented so as to maximally avoid areas of charge concentration in the distorted inner-valence shell of the chromium atoms.

I. Introduction

High-order metal−metal bonding in transition metal complexes has been a subject of ongoing experiment and theoretical study.[1−4] Different methodologies have generated differing values for bond orders and also controversy.[4−12] As of this writing, the strongest chromium−chromium bond appears to be that in the recently synthesized[13,14] dinuclear chrominum diazadiene complex (μ-η^2-$^{H}L^{iPr}$)$_2$Cr$_2$ (**1**), where $^{H}L^{iPr}$ = *N*,*N*′-bis(2,6-diisopropylphenyl)-1,4-diazadiene (see Scheme 1). The value of 1.803 Å for the Cr_2 bond distance in **1** is one of the shortest on record,[13] suggesting very strong bonding. The nature of the bonding between chromium atoms and between the chromium atoms and the two enediamide ligands in this complex is explored here by using properties of the topology of the electron density available from the quantum theory of atoms in molecules (QTAIM).[15,16] To simplify the calculations, particularly the necessary yet extensive atomic basin integrations, we use the model molecule **2**, computed by Kreisel et al.,[13] where the four diisopropylphenyl groups on the nitrogens are replaced with hydrogen atoms.

II. Methods

The wave function of **2** was computed for QTAIM analysis as a single point calculation with Gaussian03[17] at the HF/6-311G level with use of published atomic coordinates found in the Supporting Information of the work of Kreisel et al.[13] This model molecule was optimized with the above basis set with DFT(B3LYP) by Kreisel et al.[13] and produced a geometry with bond lengths and bond angles similar to the experimental values of **1** except the N_4Cr_2 core of **2** is planar, whereas in **1** it is slightly nonplanar with a ∠NCrCrN dihedral angle of ∼17°. The optimized model **2** also has a slightly shorter Cr_2 bond length of 1.764 Å. The Hartree−Fock method was used in generating the wave function since it is most appropriate for recovering the Lewis concept[18] of the electron pair, as in this case the only source of electron correlation comes from the antisymmetrization of the wave function.[19,20] The latter restriction leads to electron pairing in the ground state of closed shell molecules.

Properties of the electron density, obtained from the molecular wave function, were analyzed with QTAIM, using the AIM2000 program.[21] It is assumed that the reader is familiar with the QTAIM. For others, a more complete discussion of QTAIM is found in the Supporting Information. Localization indices of electrons in atomic basins A, λ(A), and delocalization indices between atoms A and B, δ(A,B), were calculated as described by Fradera et al.[22] and Biegler-Konig and Schonbohm.[21] These properties are based on the conditional same spin pair-probability distribution function and the spread of the Fermi hole for the same spin electrons throughout the entire molecule.[15,19,23] Occupancy of the Fermi hole for electrons of opposite spin—not excluded by antisymmetrization of the wave function—results in electron pairing.

SCHEME 1

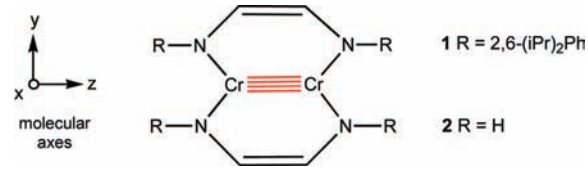

Difficulties in reproducing experimental geometries of the chromium dimer portion of molecules with single determinant wave functions have been reported.[5] DFT(B3LYP) calculations have nevertheless been used successfully with natural bond orbital[24] (NBO) calculations on a simplified model (HCrCrH) of the $Cr_2[C_6H_3$-2,6$(C_6H_3$-2,6$Pr'_2)_2]_2$ terphenyl ligand complex, where the experimental Cr_2 bond distance of the latter molecule is 0.190 Å longer than the optimized model.[15] In our case, the Cr_2 bond distance is only 0.039 Å longer in **1** than in **2**.

III. Results

1. Bonding in the Supported Cr_2 Dimer. The calculated QTAIM properties of model **2** to be discussed in this article are summarized in Tables 1−3. The integrated charges (Table 2) within the chromium and nitrogen atom basins are 1.227e and −1.266e, respectively, indicating considerable charge transfer from the chromium atoms into the neighboring nitrogens of the ligands. The overall integration error is only 0.004e over the entire complex. Regions of charge concentration (CC) and charge depletion (CD) are revealed in the Laplacian of the electron density, $\nabla^2\rho(r)$, where $\nabla^2\rho(r) < 0$ corresponds to CC and $\nabla^2\rho(r) > 0$ to CD.[15] A contour plot of $\nabla^2\rho(r)$ in the molecular plane of **2** is shown in Figure 1, where black lines delineate regions of CC and green lines, regions of CD. The plot includes an overlay of the intersection in the molecular plane of the

[†] E-mail: d.dupre@louisville.edu.

10.1021/jp808758h CCC: $40.75
Published on Web 01/30/2009

TABLE 1: Topological Properties of Bonding in Dinuclear Chromium Diazadiene Complex Model 2[j]

	Cr—Cr	Cr—N	N—C	C—C
d(Å)[a]	1.764	1.904	1.405	1.369
ρ_b[b]	0.2567	0.1273	0.2717	0.3086
$L(\rho_b)$[c]	−0.2268	−0.1096	0.1690	0.2007
$\nabla^2\rho_b$[d]	0.9072	0.4384	−0.6760	−0.8028
$G(\rho_b)$[e]	0.4328	0.1564	0.1438	0.1103
$V(\rho_b)$[f]	−0.6388	−0.2033	−0.4566	−0.4213
$H(\rho_b)$[g]	−0.2060	−0.0469	−0.3128	−0.3110
$\lambda1$[h]	−0.4198	−0.2002	−0.4935	−0.6294
$\lambda2$	−0.3904⊥	−0.1974	−0.4756⊥	−0.4825⊥
$\lambda3$	1.7174	0.8359	0.2929	0.3092
ε[i]	0.0753	0.0142	0.0376	0.3045
$G(\rho_b)/\rho_b$	1.6860	1.2286	0.5293	0.3574
$H(\rho_b)/\rho_b$	−0.8025	−0.3684	−1.1513	−1.0078
$\lvert V(\rho_b)\rvert/G(\rho_b)$	1.4760	1.2999	3.1752	3.8196

[a] d = bond distance (in Å) from X-ray structure [ref 13]. [b] b = bond critical point (bcp). [c] $L(\rho_b) = -(1/4)\nabla^2\rho_b$. [d] $\nabla^2\rho_b$, Laplacian of the electron density at the bond critical point. [e] $G(\rho_b)$, positive definite form of the electronic kinetic energy density [ref 30]. [f] $V(\rho_b)$, electronic potential energy density. [g] $H(\rho_b) = G(\rho_b) + V(\rho_b)$, total energy density at the bond critical point. [h] λi (i = 1, 2, 3), eigenvalues of the Hessian matrix, $\lambda2$ vector (major axis of ellipticity of charge contraction at ρ_b) perpendicular (⊥) to molecular plane, otherwise $\lambda2$ lies in-plane. [i] Bond ellipiticity, $\varepsilon = \lambda1/\lambda2 - 1$. [j] All quantities in atomic units (au) except for bond distances which are in Å.

TABLE 2: Integrated Atomic Charges of Model Complex 2 and Localization (λ)/Delocalization (δ) Indices for Chromium Atom

atom	charge[a]	λ, δ	index
Cr	1.227	λ(Cr)	19.996
N	−1.226	λ(N)	6.708
C	0.314	δ(Cr,Cr)	3.624
H(N)	0.310	δ(Cr,N)	0.755
H(C)	0.030	δ(Cr,N′)[b]	0.120
		δ(Cr,C)	0.038
		δ(Cr,C′)[b]	0.027
		δ(C,C)	1.646
		δ(N,C)	1.064
		δ(N,C′)[b]	0.129

[a] Integration error = 0.004e (sum of total atomic charges that should be zero). [b] N′, C′ atoms furthest removed from Cr.

interatomic surfaces (IASs) demarking the three-dimensional boundaries between adjacent atoms. Bond paths (BPs), indicated by dark lines, are present between the two chromium atoms and between chromium and the nitrogens of the ligands. The Cr—N BPs are straight lines and the angles subtended by the termination of the BPs at each nucleus are the measured geometric angles. There is, accordingly, no evidence of ring strain in the complex.

The value of 1.8028(9) Å for the Cr_2 bond distance in **1** should be compared, for example, with 1.828(2) Å found in the supported $Cr_2(2\text{-MeO-5-Me-}C_6H_3)_4$ complex synthesized in 1978 by Cotton et al.[25] and 1.8351(4) Å in the unsupported trans-bent $Cr_2[C_6H_3\text{-}2,6(C_6H_3\text{-}2,6Pr'_2)_2]_2$ terphenyl ligand complex synthesized more recently by Nguyen et al.[26] In the latter compound, 5-fold bonding interactions that are a result of 3d σ, π, and δ metal orbital overlap between the chromium atoms were determined to be present. While formally a quintuple bond, when including the effects of occupancies of antibonding MOs in a model compound, PhCrCrPh, Brynda et al.[27] calculated the theoretical effective bond order of Cr_2 to be only 3.52. Molina et al.[19] and Cortés-Guzman and Bader[28] have criticized the use of MO occupancies to determine the localization of electron pairs and the order of bonding between atoms as MOs, by their very nature, are not delimited to any set of atoms but are spread out, as the label implies, over the whole molecule. The nature of chemical bonding in the Cr_2 complex of this study will be determined here by the physics of the topology of the electron density itself—a measurable quantity.[29,30]

Figure 1 also shows that the electron density is diffuse in the outer region of the chromium atoms that, as with many electron-poor transition metal atoms,[31,32] are missing the valence shell. This is also illustrated in greater detail in Figure 3, which is a plot of $L(r) = -(1/4)\nabla^2\rho$ along the Cr_2 internuclear axis of **2** showing the atomic shell structure and lack of full condensation of the chromium valence N-shell. The bond critical point (bcp) is in fact in a region of charge depletion where $L = -0.2268$. The valence electrons for such transition metal atoms extend over the outer-valence region (missing N-shell condensation in this case) and inner-valence shell charge concentration (i-VSCC).[31,32] The value of ρ at the bcp, ρ_b, alone does not reflect the strength of this bond.[33−35] However, integration over the Cr|Cr IAS captures more of the quite diffuse, binding electron density. The value of ρ(Cr|Cr) = 1.519 is comparable to, but larger than, that found on the IASs separating Cr|N, N|C, and C|C: 0.7960, 1.270, and 1.481, respectively.

Figure 1 also shows the presence of (3, −3) charge concentrations in the i-VSCC (M-shell) of each chromium atom near, but not along, each N—Cr BP. These critical points (cps) are actually ligand opposed charge concentrations (LOCCs)[20,36,37] that result from the distortion, in the molecular plane, of the i-VSCC of the metal atom by nitrogen atoms on the *opposite* side of the complex. As shown better in the enlargement in Figure 2, these LOCCs lie along straight lines connecting each chromium nucleus with the opposing nitrogen nuclei. Also

TABLE 3: QTAIM Properties of Bonding to Transition Metal Atoms

bond	$Cr(CO)_6$ Cr—C	$(\mu\text{-}\eta^2\text{-}^H L^{iPr})_2Cr_2$ Cr—Cr	$MoCr(O_2CH)_4$ Mo—Cr	$Mo_2(O_2CH)_4$ Mo—Mo	$(W_2Cl_8)^{2-}$ W—W
references	28	this work	40	40	3
ρ_b	0.1059	0.2567	0.128	0.196	1.05
$\nabla^2\rho_b$	0.4745	0.9072	0.882	0.477	6.58
$G(\rho_b)$	0.1473	0.4328			0.97
$V(\rho_b)$	−0.1760	−0.6388			−1.47
$H(\rho_b)$	−0.0287	−0.2060			−0.50
$G(\rho_b)/\rho_b$	1.3909	1.6860	1.952	1.212	0.92
$H(\rho_b)/\rho_b$	−0.2710	−0.8025			−0.48
$\lambda1$		−0.4198	−0.079	−0.196	
$\lambda2$		−0.3904	−0.079	−0.196	
$\lambda3$		1.7174	1.040	0.869	
$\lvert V(\rho_b)\rvert/G(\rho_b)$	1.195	1.476			1.52
δ(A,B)		3.624			3.25

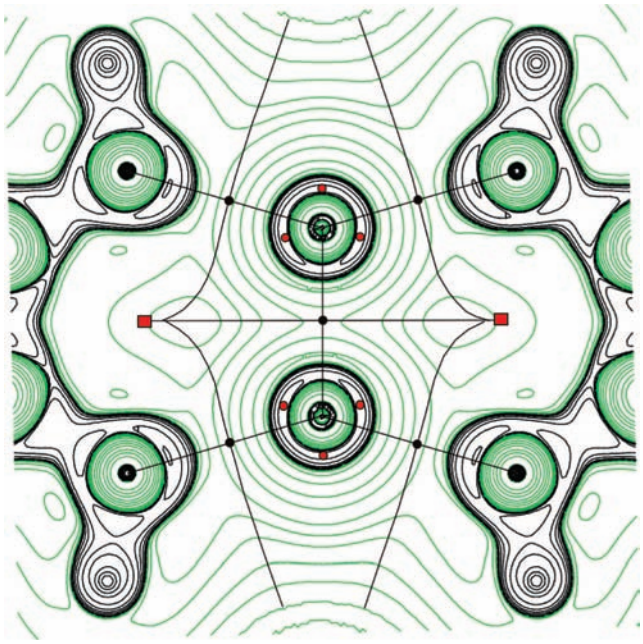

Figure 1. Contour plot of the Laplacian of the electron density ($\nabla^2\rho$) with an overlay of the projection of the interatomic surfaces (IASs)—curved lines—of each chromium atom in the plane of the molecule. Black contours are regions of charge concentration ($\nabla^2\rho < 0$); green contours are regions of charge depletion ($\nabla^2\rho > 0$). Bond paths (BPs) are indicated by straight black lines connecting chromium and nitrogen nuclear attractors. Small black circles at the intersection of BPs and the IASs are bond critical points (bcps). Small red circles in the outermost core of the chromium atoms are (3, −3) critical points of charge concentration. Red rectangles are ring critical points.

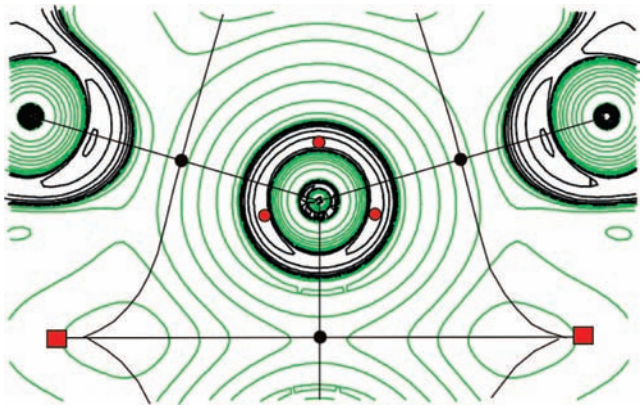

Figure 2. Enlargement of the region about one of the chromium atomic basins showing in more detail the arrangement of (3, −3) ligand opposed charge concentrations (LOCCs, red dots) in the distorted inner-valence shell charge concentration (i-VSCC) region of the metal.

notable is the absence of (3, −3) cps in the binding[38] region of the Cr_2 dimer. There are, however, two in-plane (3, −3) cps along the Cr−Cr axis in the antibinding region. The presence of these outwardly pointing CCs in the outer-core of the chromium atom is due to back-polarization resulting from the substantial, though diffuse, electron density buildup between the two chromium nuclei. An analogy in the orbital picture would be a "lost inner lobe" of the d_{z^2} orbital (along the Cr_2 axis, see Scheme 1 for the definition of the Cartesian axes) due to stresses exerted by electron−electron repulsion.

Despite falling in a region of charge depletion with $\nabla^2\rho_b > 0$, the bcp between the chromium atoms is characterized by a significantly negative value of the total electronic energy density $H(\rho_b) = G(\rho_b) + V(\rho_b) = -0.2060$, indicating that the potential

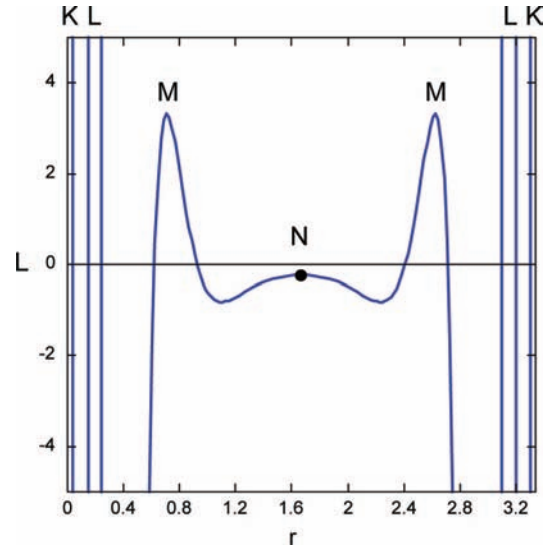

Figure 3. Plot in atomic units of $L(r) = -(1/4)\nabla^2\rho(r)$ along the Cr_2 bond path of **2** showing the atomic shell structure and lack of full condensation of the chromium outer-valence N-shell. The bond critical point (bcp), indicated by a black dot, is in a region of charge depletion where $L = -0.2268$.

energy $V(\rho_b)$ overcomes what is a large kinetic energy density per electron $G(\rho_b)/\rho_b = 1.6860$ at the bond midpoint (see data of Table 1). Furthermore, $|V(\rho_b)|/G(\rho_b) = 1.4760$ and the virial ratio of 2 is thus not met at this point. The large value of the positive eigenvalue ($\lambda 3 = 1.7174$) of the Hessian matrix at the bcp between chromium basins indicates a strong retraction of electron density out of the central binding region toward the nuclei. This dominates the significant contraction of electron density toward the Cr_2 BP found in the values of the negative eigenvalues ($\lambda 1 = -0.4198$ and $\lambda 2 = -0.3904$), resulting in a positive value of $\nabla^2\rho_b = 0.9072$. The local virial theorem[15,39] relates the scalar Laplacian, $\nabla^2\rho = \lambda 1 + \lambda 2 + \lambda 3$, to the virial of the forces acting on the electrons at a point in space through

$$(\hbar^2/4m)\nabla^2\rho(r) = 2G(r) + V(r)$$

here $V(r)$ is related to the quantum mechanical stress tensor,[15,29,30] $\vec{\vec{\sigma}}$ (a dyadic with units of pressure), and is given by:

$$V(r) = -\vec{r} \cdot \vec{\nabla} \cdot \vec{\vec{\sigma}} + \vec{\nabla} \cdot (\vec{r} \cdot \vec{\vec{\sigma}})$$

When $\lambda 3 > |\lambda 1 + \lambda 2|$, as above, $\nabla^2\rho$ is positive and there are increased stresses on the electron density in the central binding region to adapt to the virial ratio of $|V|/G = 2$ in order to minimize the increase in the kinetic energy.[40,41] A value of $|V|/G$ between 1 and 2 can be taken as being indicative of intermediate interactions.[42] Such bonds are also considered as transitional and characteristic of incipient covalent bond formation.[43] The Cr_2 bond is not cylindrical but has a slight ellipticity $\varepsilon = \lambda 1/\lambda 2 - 1$ of 0.0753; the major axis of the $\lambda 2$ eigenvector is perpendicular to the molecular plane and the bond thus displays some π-polarization.

The values of the localization λ(Cr) and delocalization δ(Cr,Cr) indices (Table 2) are of particular interest for the characterization of the Cr_2 multiple bond. Here for molecule **2**, the average number of electrons in each Cr atomic basin is found to be N(Cr) = 22.745 and as λ(Cr) = 19.996, 87.9% of these electrons remain localized. The high degree of localization of pair density within the chromium basin is remarkable, particularly considering the additional electron exchange with the atoms of the two supporting ligands. In this molecule, Δ(Cr) = N(Cr) − λ(Cr) = 2.749 electrons are delocalized among (exchanged

with) the other atomic basins of the molecule—$^1/_2 \times \delta$(Cr,Cr) = 1.812 of these with the other bonding chromium. The calculated value of δ(Cr,Cr) = 3.624 from this work is indicative of sharing of just under *four* Lewis electron pairs between the chromium atoms in the complex; i.e., the Cr_2 dimer bears nearly a *quadruple* bond. δ(Cr,Cr) is not an integral number of electrons because the remaining ~0.4 electrons are delocalized over the remaining atoms of this polyatomic molecule. The value of δ(Cr,Cr) = 3.624 is somewhat less than the bond order value of 4.28 deduced[13] for the simplified model **2** from NBO[24] and natural resonance theory (NRT).[44−46] The delocalization index, however, is obtained here by a very different physical method based upon the Pauli exclusion principle and the Fermi hole.[15,19,23]

Also instructive is a comparison of our results on Cr_2 bonding with available literature data[3,28,40] for some QTAIM properties of Cr−C single bonds and higher order Cr−Mo, Mo−Mo, and W−W interactions. Table 3 shows that ρ_b, $\nabla^2\rho_b$, and $G(\rho_b)$ are a factor of 2 to three larger in the Cr−Cr bond of **2** than in the formal single Cr−C bond of $Cr(CO)_6$. In magnitude, the potential energy $V(\rho_b)$ is, however, a factor of 4 greater, leading to a factor of 10 greater value of $H(\rho_b)$ for the Cr_2 bonding interaction. These differences befit the formal multiple bond character of Cr_2 in **2** and the single bond character of the Cr−C bond in $Cr(CO)_6$. The values of the topological properties of Cr_2 in **2** are more similar to the Mo−Cr bond of $MoCr(O_2CH)_4$ (only ρ_b, $\nabla^2\rho_b$, $G(\rho_b)/\rho_b$, and the λi eigenvalues were reported).[40] The $(W_2Cl_8)^{2-}$ complex has a formal W−W bond order of 3.5, but a delocalization index δ(W,W) of only 3.25.[3] Bonding in the tungsten dimer involves contracted 4f and even more diffuse 5d and 6s orbitals. This results in much larger values of ρ_b = 1.05 and $\nabla^2\rho_b$ = 6.58. However, $V(\rho_b)$ once again outweighs $G(\rho_b)$ and the total electronic energy density at the bcp, H_b = −0.50, is negative.

2. Bonding of the Supporting Ligands with Cr_2 in the Metal−ligand Complex. Turning to the QTAIM properties of the Cr−N bonds holding the complex together, the value of ρ_b = 0.1273 and the positive value of $\nabla^2\rho_b$ = 0.4384 are indicative of a relatively weak closed-shell interaction. The total energy density $H(\rho_b)$ = −0.0469 at the bcp is, however, negative, but only slightly so, since the potential energy density $V(\rho_b)$ = −0.2033 only barely overcomes the kinetic energy density $G(\rho_b)$ = 0.1564. In magnitude, the total energy density per electron, $H(\rho_b)/\rho_b$ = −0.3684, is the smallest of the bonds of the complex listed in Table 1. Integration of ρ(N|Cr) yields a value of 0.7960 that is, as noted above, also the smallest surface integral considered here for molecule **2**. The ρ(A|B)/ρ_b ratio is known to increase with the diffuse character of electrons involved in chemical bonding.[3] The value of ρ(N|Cr)/ρ_b = 6.253 thus indicates that the electron density of the Cr−N bond is even more diffuse than that in the core Cr_2 dimer, where ρ(Cr|Cr)/ρ_b = 5.917. (The values of ρ(A|B)/ρ_b for the N|C and C|C surfaces are 4.674 and 4.799, respectively.) The Cr−N bonds are slightly elliptical with ϵ = 0.0142 and the $\lambda 2$ eigenvector is found to lie in the molecular plane.

We can think of formation of the molecular complex **2** from two isolated diimine ligands (Scheme 2), already in the geometry of those fragments in the complex, joining the Cr_2 dimer, also already in the geometry of the complex, without electronic relaxation at first. We find that the isolated ligands in this geometry can only sustain a single bond between the two carbon atoms with the sharing of a little more than one electron pair, i.e., δ(C,C) = 1.11. The nitrogen atoms show nonbonded valence shell charge concentration (VSCC) cps in the plane of the molecule, recalling Lewis n_σ(N) lone pairs, cf. Scheme 2. Upon the formation of the complex, electronic redistribution and reorganization takes place among the three fragments. The n_σ(N) critical points bifurcate and transform into two out-of-plane nonbonded n_π(N) VSCC cps as shown in the sketch in Figure 4. These CCs on each nitrogen align with two (3, +3) cps in the π-plane of the depletion zone of the "missing" outer-valence shell charge condensation, (o-VSCC), of chromium and its associated (3, +1) saddle points in the distorted i-VSCC region. That is, it is the π-plane n_π(N) lone pair (3, −3) cps that line up with the chromium atom outer charge depletions and this back-polarization is the analogue of back-donation into formally empty metal π-type d_{xy} orbitals. The latter is a response to the large inductive effect of each nitrogen and its removal of 1.23 electrons (Table 2) from each chromium atom.

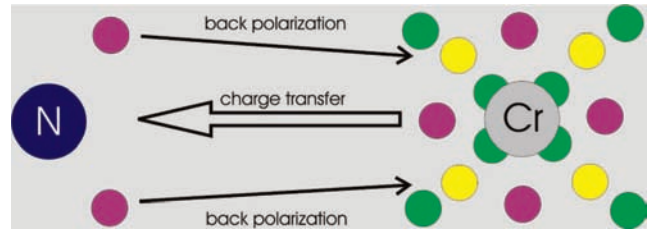

Figure 4. Sketch of the π-plane alignment of the (3, −3) valence shell charge concentrations (VSCCs, red circles) of nitrogen with (3, +3) critical points of charge depletion (green circles) in the missing N-shell region of chromium and with (3, +1) critical points of charge depletion (yellow circles) in the inner-valence shell charge concentration (i-VSCC) region of chromium. The directions of charge transfer (Cr → N) and back polarization of the nitrogen nonbonded VSCC critical points are shown with arrows.

SCHEME 2: Isolated Diimine Monomer in Geometry of the Metal−Ligand Complex (a) and Dianionic Enediamide in the Complex (b)

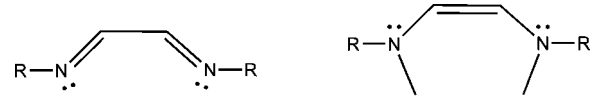

a. b.

The chemical bond of Cr_2 in the dichromium complex **2** (and by inference in the synthesized molecule **1**) may thus be summarized as follows. The electron density ρ_b at the Cr_2 bcp is relatively large, even though $\nabla^2\rho_b$ is significantly positive—an indication of substantial, though diffuse, electron density in the Cr_2 binding region. Integration of $\rho(r)$ over the Cr_2 IAS captures more of the binding density. $G(\rho_b)/\rho_b$ is large but $H(\rho_b)/\rho_b$ is negative, as $V(\rho_b)$ overcomes the destabilizing effect of the electronic kinetic energy, $G(\rho_b)$. Significant electron delocalization occurs between the chromium basins and amounts to the sharing of almost four electron pairs—i.e., according to QTAIM, an almost quadruple metal−metal bond is maintained in this complex.

On the other hand, the metal−ligand complex is held together by relatively weak ionic, dative bonds—the ionic contribution being due to a large charge transfer of 1.23e

IV. Conclusions

from the atomic basins of chromium to bonded nitrogens. There is a subsequent back-polarization of bifurcated out-of-plane n_π(N) (3, −3) cps toward charge depletion (3, +3) and (3, +1) cps in the diffuse outer-valence shell charge depletion (o-VSCD) zone (missing N-shell condensation) and in the distorted i-VSCC (M-shell), respectively. Distortion of the i-VSCC of chromium places (3, −3) CCs in and perpendicular to the molecular plane so as to maximally avoid datively bonded charge concentration of the nitrogen ligands whose (3, −3) cps are in the π-plane pointing toward chromium atom depletion cps on each side of the complex—two (3, +3) cps in the missing N-shell region and two (3 +1) cps in the chromium i-VSCC.

Acknowledgment. Supercomputer time allocations received from the University of Kentucky High Performance Computing Complex and from the Advanced Biomedical Computing Center of the Frederick Cancer Research and Development Center, National Institutes of Health are acknowledged. Support for this work also came from a Research Initiation Grant from the Office of the Vice President for Research, University of Louisville, and an Intramural Research Grant from the College of Arts and Sciences, University of Louisville. The author also gratefully acknowledges the critical reading of the manuscript by University of Louisville colleagues Craig A. Grapperhaus, Lucius E. Johnson, and M. Cecilia Yappert.

Supporting Information Available: Complete author list for ref 17 and a more detailed narrative about QTAIM methodology. This material is available free of charge via the Internet at http://pubs.acs.org.

References and Notes

(1) Cotton. F. A.; Murillo, C. A.; Walton, R. A. *Multiple Bonds Between Metal Atoms*, 3rd ed.; Springer: New York, 2005.
(2) Chisholm, M. H.; Macintosh, A. M. *Chem. Rev.* **2005**, *105*, 2949–2976.
(3) Macchi, P.; Sironi, A. *Coord. Chem. Rev.* **2003**, *238*−*239*, 383–412.
(4) Power, P. P. *Chem. Rev.* **1999**, *99*, 3463–3503.
(5) Landis, C. R.; Weinhold, F. *J. Am. Chem. Soc.* **2006**, *128*, 7335–7345.
(6) Xe, Y.; Schaefer, H. F., III.; Robinson, G. H. *Chem. Phys. Lett.* **2000**, *317*, 174–180.
(7) Michalak, A.; DeKock, R. L.; Ziegler, T. *J. Phys. Chem. A* **2008**, *112*, 7256–7263.
(8) Krapp, A.; Lein, M.; Frenking, G. *Theor. Chem. Acc.* **2008**, *120*, 313–320.
(9) Frenking, G. *Science* **2005**, *310*, 796–797.
(10) Gagliardi, L.; Roos, B. O. *Inorg. Chem.* **2003**, *42*, 1599–1603.
(11) Ponec, R.; Yuzhakov, G. *Theor. Chem. Acc.* **2007**, *118*, 791–797.
(12) Andersson, K., Jr.; Persson, B. J.; Roos, B. O. *Chem. Phys. Lett.* **1996**, *257*, 238–248.
(13) Kreisel, K. A.; Yap, G. P. A.; Dmitrenko, O.; Landis, C. R.; Theopold, K. H. *J. Am. Chem. Soc.* **2007**, *129*, 14162–14163.
(14) *C&E News* **2007**, *Nov. 19*, 52−53.
(15) Bader, R. F. W. *Atoms in molecules. A quantum theory*; Clarendon Press: Oxford, UK, 1990.
(16) Popelier, P. *Atoms in molecules. An introduction*; Prentice Hall: New York, 2000.
(17) Frisch, M. J. et al. *Gaussian03*, Revision C.02; Gaussian, Inc.: Wallingford, CT, 2004.
(18) Lewis, G. N. *J. Am. Chem. Soc.* **1916**, *38*, 762–785.
(19) Molina, J. M.; Dobado, J. A.; Heard, G. L.; Bader, R. F. W.; Sundberg, M. R. *Theor. Chem. Acc.* **2001**, *105*, 365–373.
(20) Bader, R. F. W.; Gillespie, R. J.; Martin, F. *Chem. Phys. Lett.* **1998**, *290*, 488–494.
(21) Biegler-Konig, F.; Schonbohm, J. *J. Comput. Chem.* **2002**, *23*, 1489–1494.
(22) Fradera, X.; Austen, M. A.; Bader, R. F. W. *J. Phys. Chem. A.* **1999**, *103*, 304–314.
(23) Bader, R. F. W.; Johnson, S.; Tang, T.-H.; Popelier, P. L. A. *J. Phys. Chem.* **1996**, *100*, 15398–15415.
(24) Reed, A. E.; Curtiss, L. A.; Weinhold, F. *Chem. Rev.* **1988**, *88*, 899–926.
(25) Cotton, F. A.; Koch, S. A.; Millar, M. *Inorg. Chem.* **1978**, *17*, 2084–2086.
(26) Nguyen, T.; Sutton, A. D.; Brynda, M.; Fettinger, J. C.; Long, G. J.; Power, P. P. *Science* **2005**, *310*, 844–847.
(27) Brynda, M.; Gagliardi, L.; Widmark, P.-O.; Power, P. P.; Roos, B. O. *Angew. Chem., Int. Ed.* **2006**, *45*, 3804–3807.
(28) Cortés-Guzman, F.; Bader, R. F. W. *Coord. Chem. Rev.* **2005**, *249*, 633–662.
(29) Bader, R. F. W. *Monatsh. Chem.* **2005**, *136*, 819–854.
(30) Bader, R. F. W. *J. Phys. Chem. A* **2007**, *111*, 7966–7972.
(31) MacDougall, P. J.; Hall, M. B. *Trans. Am. Crystallogr. Assoc.* **1993**, *26*, 105–123.
(32) MacDougall, P. J.; Hall, M. B.; Bader, R. F. W.; Cheeseman, J. R. *Can. J. Chem.* **1989**, *67*, 1842–1846.
(33) Macchi, P.; Proserpio, D. M.; Sironi, A. *J. Am. Chem. Soc.* **1998**, *120*, 13429–13435.
(34) Cremer, D.; Kraka, E. *Croat. Chem. Acta* **1984**, *57*, 1259–1281.
(35) Cremer, D.; Kraka, E. *Angew. Chem., Int. Engl. Ed.* **1984**, *23*, 627–628.
(36) Bytheway, I.; Gillespie, R. J.; Tang, T.-H.; Bader, R. F. W. *Inorg. Chem.* **1995**, *34*, 2407–2414.
(37) Gillespie, R. J.; Bytheway, I.; Tang, T.-H.; Bader, R. F. W. *Inorg. Chem.* **1996**, *35*, 3954–3963.
(38) Berlin, T. *J. Chem. Phys.* **1951**, *19*, 208–213.
(39) Bader, R. F. W. *Chem. Eur. J.* **2006**, *12*, 7769–7772.
(40) Sierraalta, A. *Chem. Phys. Lett.* **1994**, *227*, 557–560.
(41) Bader, R. F. W.; Preston, H. J. T. *Int. J. Quantum Chem.* **1969**, *3*, 327–347.
(42) Espinosa, E.; Alkorta, I.; Elguero, J.; Molin, E. *J. Chem. Phys.* **2002**, *117*, 5529–5542.
(43) Gatti, C.; Lasi, D. *Faraday Discuss.* **2007**, *135*, 55–78.
(44) Glendening, E. D.; Weinhold, F. *J. Comput. Chem.* **1998**, *19*, 593–609.
(45) Glendening, E. D.; Weinhold, F. *J. Comput. Chem.* **1998**, *19*, 610–627.
(46) Glendening, E. D.; Badenhoop, J. K.; Weinhold, F. *J. Comput. Chem.* **1998**, *19*, 628–646.

JP808758H